NASA Technical Memorandum 82699

Effects of Fan Inlet Temperature Disturbances on the Stability of a Turbofan Engine

Mahmood Abdelwahab
Lewis Research Center
Cleveland, Ohio

December 1981

NASA

EFFECTS OF FAN INLET TEMPERATURE DISTURBANCES ON THE STABILITY OF A TURBOFAN ENGINE

by Mahmood Abdelwahab

National Aeronautics and Space Administration
Lewis Research Center
Cleveland, Ohio

SUMMARY

An experimental investigation was conducted to determine the effects of steady-state and time-dependent fan inlet total temperature disturbances on the stability of a TF30-P-3 turbofan engine. Disturbances were induced by a gaseous-hydrogen-fueled burner system installed upstream of the fan inlet. Data were obtained at a fan inlet Reynolds number index of 0.50 and at a low-pressure-rotor corrected speed of 90 percent of military speed. All tests were conducted with a 90° extent of the fan inlet circumference exposed to above-average temperatures.

During increasing levels of fan inlet steady-state temperature distortion, stall began in the high-pressure compressor when a critical stage reached its stall temperature-rise limit. This limit was represented at the fan inlet by the magnitude of 67 K.

During time-dependent disturbances the hydrogen burner system produced transients with the following characteristics: (1) fan inlet temperature-rise rates and magnitudes as high as 20 000 K/sec and 300 K, respectively, (2) approximately the same rise magnitude but different rise rates or conversely, and (3) peak inlet temperature rise occurring before or after stall.

The compressor system response to fan inlet temperature transients with low rates and magnitudes was similar to the steady-state response in that stall began in the high-pressure compressor. At very high rise rates and rise magnitudes, stall began in the low-pressure compressor.

For the hydrogen burner system used in this experiment a 94 K threshold level of instantaneous, spatial, average fan inlet temperature rise was required to stall the compressor. The results indicate that the temperature-rise limit required to stall the compressor was independent of the rise rate. In terms of the cumulative, average, fan inlet temperature rise the threshold level of temperature rise for stall was independent of the time required to stall and equal to the steady-state level of 67 K. The cumulative average indicates the net change (time dependence) in the instantaneous spatial average from the initial temperature rise to the time of stall.

INTRODUCTION

An experimental investigation was conducted to determine the effects of both steady-state and time-dependent fan inlet total-temperature disturbances on the stability limits of a production TF30-P-3 turbofan engine. Typically these types of disturbances at the engine inlet can occur as a result of hot-gas ingestion by the engine during, for example, armament firing, thrust reversal, and takeoff and landing by VTOL and STOL aircraft. Although the total problem of hot-gas ingestion is very complex and involves many factors,

temperature distortion is probably the principal factor affecting the performance and stability limits of the engine. Therefore an investigation of the isolated effects of temperature distortion on engines will add to the knowledge and understanding of the total problem of ingestion and could provide information leading to its alleviation and/or elimination.

Most earlier investigations of engine inlet temperature disturbances were conducted on turbojet engines and were concerned with either steady-state or time-dependent disturbances (refs. 1 and 2). Recently some reports were published concerning the effects of either steady-state or time-dependent temperature disturbances on turbofan engines (refs. 3 and 4). In reference 4, where the investigation of time-dependent temperature disturbances was conducted on the same engine used for this investigation, the data suggested strongly that compressor stability limits during fan inlet temperature transients were a function of the critical magnitude of the fan inlet temperature rise and were independent of the temperature-rise rate. The investigation reported herein was conducted to further extend our knowledge of the interdependence of these fan inlet temperature variables and to explore the relationship between them during steady-state and time-dependent disturbances.

The experiment was conducted in a NASA Lewis altitude test facility on a twin-spool, low-bypass-ratio turbofan engine equipped with an afterburner. Temperature disturbances were generated by a gaseous-hydrogen-fueled burner installed upstream of the engine inlet. The transients were controlled by varying the flow rate and amount of a trapped volume of hydrogen and thus varying the magnitude and rate of the inlet temperature change. To some extent the period of the transients was also varied by changing the size of the trapped hydrogen volume. The steady-state stall limits were obtained by slowly increasing the hydrogen flow rate, and thus the fan inlet temperature rise, until stall occurred. Data were obtained at a fan inlet Reynolds number index of 0.50 and at 90 percent of the low-pressure-rotor military speed. Distortion was imposed on only 90° of the fan inlet circumference.

APPARATUS

Engine

The engine used for this investigation was a production TF30-P-3 (serial number P-658929), twin-spool turbofan engine equipped with an afterburner and 7th and 12th stage compressor bleeds. The engine was installed in a NASA altitude test chamber by a direct-connect type of installation (fig. 1).

Distortion Device

The gaseous-hydrogen-fueled burner used to produce the steady-state and time-dependent temperature disturbances was installed upstream of the inlet bellmouth (fig. 2). The burner duct was divided into four quadrants (figs. 3 and 4) and could be positioned ±30° off the vertical centerline. Air passing through the burner was heated in selected 90° sectors. Each 90° sector of the burner consisted of five swirl-can pilot burners that provided the ignition source for the hydrogen, five annular gutters supported by one radial gutter, and five circular tube manifolds (one inside each annular gutter) with small holes for hydrogen injection. These circular tubes were linked by tubing to a circular manifold located on the outside of the burner duct (fig. 5(a)).

During transients the solenoid-actuated valve (called fire valve B in figs. 3 and 5(a)) located on this manifold was connected to the variable-volume pipe (figs. 3 and 5(a)) by flexible tubing. The pipe consisted of a high-response pneumatically controlled valve (referred to as fire valve A in figs. 3 and 5(a)) and a 5.08-cm-inside-diameter pipe divided into seven volumes of 410, 410, 410, 820, 820, 820, and 1229 cm^3. The variable-volume pipe was linked to a 324-N/cm^2 gaseous hydrogen source that was regulated to a specified pressure by a pressure regulator. During testing, either fire valve A or B was closed, and hydrogen was trapped in a specified volume by closing one of the seven solenoid-actuated valves in the variable-volume pipe.

During steady-state distortion tests a large circular manifold located on the outside of the bellmouth (fig. 5(b)) was connected to each of the burner sectors through a flow control valve by flexible tubing. The manifold was linked to the gaseous hydrogen supply source through the variable-volume pipe.

Instrumentation

The engine was instrumented as shown in figure 2. Steady-state and dynamic total pressure, static pressure, and total temperature were measured and recorded. Steady-state pressures were measured by means of a strain-gage transducer system. Steady-state temperatures were measured by using Chromel-Alumel thermocouples.

Dynamic pressure measurements were made by using miniature strain-gage transducer rakes capable of at least 300-Hz frequency response. A more complete discussion of this type of instrumentation is given in reference 5. Chromel-Alumel thermocouples made from 0.076-mm-diameter wires were used throughout the engine (fig. 2) to measure the transient total temperature. The indicated temperatures from these thermocouples were corrected for ram recovery and time lag on the basis of steady-state data recorded before each transient. The methods used for these corrections are given in appendix B. (Symbols are defined in appendix A.) During the course of the experiment the circumferential locations of the pressure and temperature rakes at stations 2A and 2 (fig. 2) were rearranged to provide better fan inlet, total temperature, spatial (radial and circumferential) profile definitions in the burner fourth quadrant, where most of the time-dependent temperature distortion occurred.

The gaseous-hydrogen-burner instrumentation layout is shown in figure 3. This instrumentation consisted of high-response pressure transducers to measure the gaseous hydrogen volume pressure and to define the pressure profiles just upstream of the injection holes.

The high-response pressure and temperature measurements were recorded on an analog recording system. The data were digitized at a rate of 1000 samples per second. A 500-Hz low-pass filter was used prior to digitization. Selected dynamic measurements were recorded and digitized on a high-speed sequential digital system at a rate of 435 samples per second per channel for the purpose of on-line data reduction and analysis.

PROCEDURE

For this investigation the fan inlet pressure and temperature were set before taking each data point to obtain a fan inlet Reynolds number of 0.50. The fan inlet temperature prior to distortion was set at approximately 289 K.

Tests were conducted at a predistortion fan corrected speed of 8600 rpm. Only 90° circumferential extents of the fan inlet were exposed to distortion.

Steady-State Disturbances

The purpose of this procedure was to determine the fan inlet and compressor interstage temperature-rise limits during steady-state, 90° circumferential-extent temperature distortion. To do this, the line connecting the variable-volume pipe to the large manifold on the outside of the bellmouth duct was installed. The pilot system was activated and the swirl-can ignitors were then lit. Fire valves A and B were opened. Gaseous hydrogen was then supplied to the five gutters of a specific quadrant through the flow control valve until the whole quadrant was lit. The flow control valve was then opened until the fan inlet temperature was just below the expected stall limit. A steady-state data point was recorded and the high-speed data systems were activated. The flow control valve was then slowly opened, raising the fan inlet temperature, until the engine stalled. This procedure was repeated in each of the four fan inlet quadrants to obtain compressor interstage temperature rise at stall. It was necessary to map the interstages circumferential profiles since only one temperature rake was installed in each interstage.

Time-Dependent Disturbances

The purpose of this procedure is to vary fan inlet temperature-rise rate and magnitude independently by varying the size and pressure of a trapped gaseous hydrogen volume. The line connecting the variable volume to the gaseous hydrogen manifold used during steady-state distortion was disconnected, and flexible tubing was used to connect a specified quadrant to the variable-volume pipe (fig. 5(a)). Several configurations of the gaseous hydrogen burner system were used to generate the temperature transients. These configurations are listed in table I as experiments 1 to 16. Temperature transients were produced by using the following procedure: For a specified burner quadrant, either fire valve A or B was closed. The line between the specified fire valve and the gaseous-hydrogen-source pressure regulator (fig. 3) was charged to a predetermined hydrogen pressure level. Depending on the specified volume, one of the seven valves in the variable-volume pipe was closed, and thus hydrogen was trapped between that valve and the fire valve. A steady-state data point was recorded when all test conditions had been stabilized. The swirl-can ignitors in the quadrant were then lit. The high-speed data systems were activated and the specified fire valve was remotely opened. The trapped hydrogen was burned, giving a specific temperature rise and rise rate in the specified 90° sector of the burner. Depending on whether compressor stall occurred, the gaseous hydrogen pressure was increased or decreased and the process was repeated until the minimum gaseous hydrogen pressure level required for stall was reached. The same procedure was repeated for different quadrants of the burner and for different trapped hydrogen volumes and pressures. A special gaseous hydrogen line was installed (fig. 3) so that all four quadrants, in addition to the pilots, would be lit prior to a transient, thus assuring the complete burning of all gaseous hydrogen during the transient. This was done only for experiments 9 and 10 (table I) and resulted in a pretransient fan inlet temperature of 300 K as compared with 289 K for all other experiments.

RESULTS AND DISCUSSION

The effects of both steady-state and time-dependent fan inlet temperature disturbances were investigated at a fan inlet Reynolds number index of 0.50 and at a low-pressure-rotor speed of 8600 rpm. Tests were conducted with a 90° circumferential extent of the fan inlet exposed to distortion. The results of the steady-state disturbance are discussed herein in terms of the type of compression system response and the magnitude of the temperature rise required to stall the compressor system. The effects of time-dependent temperature disturbances are presented and discussed under three categories: (1) fan inlet flow conditions during the transients and prior to compressor stall, (2) engine response, and (3) compressor distortion limits and their relation to the steady-state limits.

Steady-State Temperature Disturbance

Engine response. - A typical example of time histories of engine pressures during steady-state temperature distortion to stall is presented in figure 6. Pressure fluctuations are evident in the right and left sides of the engine as indicated by the total and static pressures at stations 2.3, 2.6, 3, 3.12, and 4 prior to the start of fan inlet (station 2) hammershock. As reported in reference 6 the sign of these fluctuations provides evidence of the stall-initiating stage. Pressure increases (positive fluctuations) are normally observed at measuring stations upstream of the stall; pressure decreases occur downstream. According to this criterion, the data in figure 6 indicate the location of the initial instability to be between station 3.12 (middle of the high-pressure compressor) and station 3 (exit of the low-pressure compressor). Evidence of this is shown by the negative pressure fluctuations downstream of station 3.12 and the positive pressure fluctuations upstream of station 3. Complete compressor stall followed the initial instability, starting in the high-pressure compressor and progressing to the upstream and downstream stages, as shown by the sudden sequential increase or decrease in pressure at stations 4 ($t = 80$) to 2.3 ($t = 83$).

Compressor distortion limits. - The steady-state temperature distortion limits are given in figure 7. Plotted is the limiting temperature rise at each compressor station. The rise limit at each station was calculated as the difference between the temperature level occurring just prior to the station's sudden pressure increase or decrease, indicating complete stall, and the pre-distortion level. The limiting 67 K rise at the fan inlet was calculated as the average of probe positions 3 and 4 for rakes at relative locations of 15° and 60°. However, this limit varied locally from a high of 76 K (indicated by probe 3) to a low of 49 K (indicated by probe 5). The corresponding limiting temperature rises at stations 2.1, 2.3, 2.6, 3, and 4 shown in the figure were obtained from probe position 3; station 3.12 data were obtained from probe position 1. It is evident from these data that the limiting level of temperature rise at any compressor interstage was essentially between the maximum and minimum of the fan inlet temperature rise, with the exception of station 4, which showed higher results. These higher results are probably due to the limited circumferential temperature coverage.

In summary, for steady-state temperature disturbances the temperature rise required to stall the compressor was 67 K. This limit remained approximately unchanged as the heated gases traveled through the machine. It represents the

temperature rise stall limit for a critical stage located in the rear of the compressor system in the high-pressure compressor.

Time-Dependent Temperature Disturbances

Fan inlet conditions. - To better understand the effects of time-dependent temperature disturbances produced by the gaseous hydrogen burner system on engine stability, the fan inlet flow conditions during the transients and prior to compressor stall should be defined. These conditions serve to identify the inlet variables affecting the engine response and its tolerance to distortion. For this purpose, data are presented to show the instantaneous variations in fan inlet temperature and pressure during a transient and prior to stall. Also, the effects of the gaseous hydrogen burner system parameters (volume and pressure) on the temperature pulse characteristics are discussed.

A typical example of fan inlet temperature transient during which stall occurred is presented in figure 8. Time histories are shown of gaseous hydrogen volume pressure, selected segment pressures, and average corrected and indicated fan inlet temperature. The temperature plotted is the average of all five radial probes at relative circumferential locations of 27°, 45°, and 65° (experiment 9, table I) in the heated quadrant. Gaseous hydrogen pressure-time histories indicate that the pressure upstream of the injection holes (indicated in fig. 8 as gaseous hydrogen gutter segment pressure) was uniform in the three gutter segments in terms of the initial time of pressure rise. However, pressure-rise rate and maximum rise magnitude, which are directly related to fan inlet temperature-rise rate and magnitude, respectively, were not uniform. The middle gutter segment (3) showed the highest values of pressure-rise rate and magnitude. The resultant time history of circumferential and radial fan inlet temperature for this test point is presented in figure 9. The circumferential temperature profiles (fig. 9(a)) represent data obtained from the middle thermocouple probe (probe 3) of each fan inlet temperature rake (configuration I, fig. 2). The radial profiles (fig. 9(b)) represent data obtained from the individual probes of the rake at a relative angular location of 45°. It is apparent from these profiles that the time-dependent temperature distortion produced by the hydrogen burner system contained circumferential and radial variations in temperature-rise rate, as well as instantaneous spatial temperature distortion, prior to compressor stall (indicated in figure 9 by the time of the start of the hammershock at the fan inlet). For example, the temperature-rise rate varied circumferentially from 2038 K/sec at $\theta = 90°$ to 3172 K/sec at $\theta = 63°$. It varied radially from 1094 K/sec at an inlet passage height of 92.2 percent (probe 1 tip) to 3230 K/sec at 41.8 percent. These rise rates represent the initial, nearly linear, maximum temperature-rise rate calculated as the slope of a straight-line least-squares curve fit of the first 15 to 20 time points (time point = 0.001 sec) after the first indication of temperature rise. This rate is referred to throughout this report as the fan inlet, initial, maximum temperature-rise rate. The absolute value of instantaneous temperature, for example, at t = 45 msec, varied circumferentially from 350 K at $\theta = 90°$ to 393 K at $\theta = 63°$ and radially from 333 K at an inlet passage height of 92.2 percent to 394 K at 41.8 percent. The data also show slight variations radially and circumferentially in the initial time of temperature rise. The minimum variations in temperature-rise magnitude and rate were indicated by the third and fourth radial probes for rakes with angular locations less than

90° and more than 0° in the heated quadrant. Although not shown, similar profiles were obtained from all other experiments. Therefore, in all subsequent discussions, fan inlet parameters (temperature rise and rise rate) are represented by data obtained from these probe positions and angular locations.

Time histories of fan inlet total and static pressures during transients are given in figure 10. To obtain a wide range of circumferential and radial profiles in the heated quadrant, data from several test experiments obtained during testing in the first, second, third, and fourth fan inlet quadrants were used. The data indicate no appreciable circumferential or radial pressure variations during transients prior to stall.

The type of temperature pulse imposed on the fan inlet is a function of the initial pressure and volume size of the trapped gaseous hydrogen. With certain combinations of hydrogen pressure and volume, the gaseous hydrogen system imposed temperature pulses on the engine inlet that had approximately the same temperature rise but different rise rates (fig. 11(b)) or conversely (fig. 11(a)). Also, with respect to compressor stall time, which is defined throughout this report as 0.003 sec prior to the time of peak fan discharge pressure, two pulse characteristics were identified. The first is defined by a peak, instantaneous, fan inlet temperature occurring much before the stall time and remaining approximately constant until stall (fig. 12, solid-line curve). This type of characteristic occurred at low and moderate trapped-hydrogen pressures, but above that required for stall, regardless of the size of the hydrogen volume. The second type is characterized by a peak instantaneous temperature occurring at or after stall (fig. 12, dashed-line curve). It occurred with very high trapped-hydrogen pressure.

In summary, the gaseous hydrogen burner system delivered heated air to the fan inlet in the following conditions: (1) spatial distortion in the temperature within the heated sector, (2) radial and circumferential variation in the temperature-rise rate, and (3) no appreciable variations in the total or static pressure prior to stall. Also, the system produced transients with the following characteristics: (1) the same rise magnitude but different rise rates or the same rise rate but different rise magnitudes, and (2) a peak fan inlet temperature occurring before or after stall.

Engine response. - The response of the compression system to fan inlet time-dependent temperature disturbances as produced by the hydrogen burner system is dependent on the severity of the disturbances as defined by the rise rate and rise magnitude of the fan inlet temperature. The response could be characterized by (1) no stall, (2) stall that starts in the high-pressure compressor, and (3) stall that starts in the low-pressure compressor. A typical example of each response is shown in figures 13, 14, and 15 in terms of time histories of fan inlet and compression system interstage pressures during distortion and up to and including complete compressor stall. Engine pressures indicate that no major activities were occurring during no-stall transients (fig. 13), that is, during transients whose fan inlet temperature-rise rate and magnitude were below the threshold levels required to stall the engine (see the following section Compressor distortion limits). A further increase above these threshold levels resulted in a high-pressure-compressor-initiated stall (fig. 14). This response is similar to that obtained during steady-state temperature distortion to stall (fig. 6) in that positive pressure fluctuations were observed only at or upstream of station 3 ($P_{s,3-81°}$), an indication that the stall-initiating stage was in the high-pressure compressor. Very high fan inlet temperature-rise rates and magnitudes caused

the low-pressure compressor to stall first, as is evident by the negative pressure fluctuations indicated by pressures at or downstream of station 2.3 in figure 15. Although engine speeds are not shown in these figures, they did not vary during a transient until the compressor stalled.

The change in the stall-initiating stage from the high-pressure compressor at low fan inlet temperature-rise rates and magnitudes to the low-pressure compressor at high rise rates and magnitudes is due to the rear stages of the compressor system operating closer to their stall line at relatively high rotor speeds. Thus only a small ΔT rise is required to stall them. However, at the very high rise rates and magnitudes a front stage can reach its required level of ΔT to stall before the more critical high-pressure compressor stage has a chance to sense the full effect of the transients. Further explanation is given in the following section.

Compressor distortion limits. - The engine tolerance to time-dependent temperature distortion as characterized by compressor stall is presented in figure 16. Plotted are the fan inlet instantaneous, spatial average temperature rise $(\Delta T)_2$ against the fan inlet, initial, maximum temperature-rise rate $(\Delta T/\Delta t)_2$. Maximum fan inlet temperature rise prior to stall (tailed solid symbols) and temperature rise at stall (solid symbols) are shown for transients that resulted in stall. Only the maximum temperature rise is shown for no stall transients. The data show that in this experiment a threshold level $(\Delta T)_2$ of 94 K was required to stall the compression system. The corresponding threshold level of $(\Delta T/\Delta t)_2$ was approximately 3900 K/sec. Because of the large number of experiments and thus data points, only data from experiments 1 to 7 were used in figure 16 and all subsequent figures. The results from experiments 8 to 16 were identical to those from 1 to 7, except for slight differences due to the variations in the number of temperature rakes and the initial level of fan inlet temperature, as discussed in the section PROCEDURE.

The data in figure 16 also show that, for transients where the maximum temperature-rise magnitude was equal to but not greater than the threshold level of 94 K, the temperature-rise rate $(\Delta T/\Delta t)_2$ ranged from 3900 K/sec to 6700 K/sec. This implies that the compressor system stall is independent of $(\Delta T/\Delta t)_2$ when the magnitude of $(\Delta T)_2$ is 94 K. The increase in temperature rise for transients producing higher $(\Delta T)_2$ than 94 K at stall represents the increase in fan inlet temperature at the given rate during the time required for the pulse to go from the fan inlet to the critical stage. For this engine the time required by a particle to go from the fan inlet to the compressor exit was calculated to be approximately 0.006 sec. This observation is consistent with the slope of the line representing all stall data points as indicated in figure 16 and supports the conclusion that the critical stage is located in the rear of the compressor system. This location of the critical stage was shown, in the section Engine Response, to be true for transients with low fan inlet temperature-rise rate.

It was also previously shown that, for high $(\Delta T/\Delta t)_2$, stall started in the low-pressure compressor. This would imply a change in the slope of the line in figure 16 to a lower value for very high $(\Delta T/\Delta t)_2$. This change in slope, however, would be very small, and with the limited number of very high $(\Delta T/\Delta t)_2$ test points it was not observed. However, evidence of this change in slope is shown in figure 17, where the instantaneous temperature rise at stall at the compressor interstages is plotted against $(\Delta T/\Delta t)_2$. For very high $(\Delta T/\Delta t)_2$ the slope of the line representing the stall data points

changed from positive at the front stages (station 2.3) to negative at the rear stages (station 4). This implies that for these rates the rear stages never sense the full effect of the transients since a front stage has reached its temperature-rise limit first and causes the compressor to stall.

The steady-state temperature rise required for stall is shown in figure 16 as the temperature rise required for stall at 0 K/sec (denoted by symbol x). The steady-state distortion limit of 67 K is lower than the threshold level of 94 K required for time-dependent distortion. A better correlation of the relationship between steady-state and time-dependent distortion limits for this engine was obtained by using the cumulative time average of $(\Delta T)_2$, hereinafter referred to as $(\Delta T)_{2,ca}$ (fig. 18). The term $(\Delta T)_{2,ca}$ represents the net change (time dependence) of $(\Delta T)_2$ during a time period and was calculated as follows:

$$(\Delta T)_{2,ca} = \frac{\Delta t}{(t_f - t_0)} \sum_{\substack{(\Delta T)_2, \\ t=t_0}}^{\substack{(\Delta T)_2, \\ t=t_f}} (\Delta T)_2$$

where

t_0 time corresponding to initial temperature rise
t_f time at stall for stall transients or time at maximum $(\Delta T)_{2,ca}$ for no stall transients
Δt time interval between consecutive $(\Delta T)_2$'s (0.001 sec)
$(\Delta T)_2$ instantaneous spatial average of fan inlet temperature rise in the heated quadrant

The steady-state distortion limit of 67 K is shown in figure 18 by the dashed line. The data in this figure indicate that the critical $(\Delta T)_{2,ca}$ (shown by the solid symbols) is essentially independent of time and approximately equal to the steady-state limit of 67 K except for very high rise rates and rise magnitudes, where the critical level will change to a higher value because the location of the critical component in the compressor system changes from the high-pressure compressor to the low-pressure compressor, as explained in the section Engine response. Also, the cumulative time average $(\Delta T)_{2,ca}$ when plotted against an effective temperature-rise rate defined as $(\Delta T)_{2,ca}/\Delta t$ appears to give a more informative representation of the distortion limits, as shown in figure 19. The slope of the line representing the time it takes a particle to go from the inlet to the exit remained approximately the same as that shown in figure 16. However, the temperature-rise threshold level now corresponds to that for steady-state distortion (fig. 19).

Further evidence of the time independence of the critical fan inlet temperature-rise limit is provided when the stall development time is plotted against the effective fan inlet temperature-rise rate (fig. 20). Stall development time is defined as the time difference between the time at stall and the time at which $(\Delta T)_{2,ca}$ reached the steady-state temperature-rise limit of 67 K. The data indicate this time to be independent of the rise

rate, with a mean level of 9 msec, which for the engine speed tested corresponds approximately to two high-pressure compressor (9 msec) or two low-pressure compressor (14 msec) rotor revolutions. Since a stall front propagates around the compressor annulus at approximately 1/2 rotor speed, this is reasonable time for a stall to develop in the compressor system after the critical fan inlet temperature rise $(\Delta T)_{2,ca}$ is reached.

SUMMARY OF RESULTS

An experimental investigation was conducted to determine the effects of fan inlet total-temperature disturbance, both steady state and time dependent, on the stability of a TF30-P-3 turbofan engine. Disturbances were produced by a gaseous-hydrogen-fueled burner system installed upstream of the fan inlet. Data were obtained at a fan inlet Reynolds number index of 0.50 and at a low-pressure-rotor corrected speed of 8600 rpm. All tests were conducted with a 90° extent of the fan inlet circumference exposed to temperature distortion (i.e., above-average temperature). The following results were obtained:

1. During steady-state temperature disturbance the magnitude of the fan inlet temperature-rise limit was 67 K. The response of the compressor system was characterized by a critical stage in the rear of the compressor (the high-pressure compressor) reaching its stall temperature rise and causing the system to stall.

2. During time-dependent disturbances a 94 K threshold level of instantaneous fan inlet temperature rise was required to stall the compressor. The corresponding threshold of fan inlet, initial, maximum temperature-rise rate was 3900 K/sec. However, stall occurred where the maximum rise rate ranged from 3900 K/sec to 6700 K/sec. This would imply that the limit of 94 K was independent of the rise rate.

3. In terms of the cumulative time average of fan inlet temperature rise, the threshold level during time-dependent distortion was independent of time and approximately equal to the steady-state temperature-rise limit of 67 K.

4. The compressor system response to time-dependent fan inlet temperature distortion with low rise rates and magnitudes was similar to the steady-state response in that stall started in a high-pressure compressor stage. At very high rise rates and rise magnitudes, stall began in the low-pressure compressor.

5. The gaseous hydrogen burner system was capable of producing transients with (1) approximately the same rise magnitude but different rise rates or the same rise rate but different rise magnitudes, and (2) a peak fan inlet temperature occurring before or after stall.

6. Instantaneous spatial (circumferential and radial) distortion in the magnitude and rate of fan inlet temperature rise always accompanied the temperature transients and was primarily due to the hydrogen burner system design.

APPENDIX A

SYMBOLS

L	axial distance, cm
M	Mach number
P	total pressure, N/cm^2
P_s	static pressure, N/cm^2
R	ram recovery parameter, $1/(1 - X)$
RNI	Reynolds number index, $(P/P_{sl})(\mu/\mu_{sl})(T/T_{sl})$
T	total temperature, K
X	ram recovery factor
t	time, msec
θ	angular location, clockwise from top dead center looking forward, deg
μ	absolute viscosity, kg/m-sec
τ	time constant, sec
τ_0	reference time constant for particular probe, sec

Subscripts:

av	average
ca	cumulative average
corr	corrected
ind	indicated thermocouple reading
s	static conditions
seg	gaseous hydrogen segment
sl	sea level
t	time
vol	gaseous hydrogen volume
1	airflow-metering station
2	fan inlet temperature-measuring plane
2A	fan inlet pressure-measuring plane
2.3	fan hub exit
2.3F	fan tip exit
2.6	middle of low-pressure compressor (6th-stage stator)
3	low-pressure compressor exit; high-pressure compressor inlet
3.12	middle of high-pressure compressor (12th-stage stator)
4	high-pressure compressor exit

APPENDIX B

TEMPERATURE CORRECTION

Total temperature was measured during steady-state and time-dependent temperature distortion by bare-wire thermocouples with 0.076-mm-diameter wire. The data were recorded on an analog system and were digitized at a rate of 1000 samples per second. The digitized temperature data from each individual channel were then smoothed by performing a "running" average over a period of 0.005 sec. The running average replaced the instantaneous indicated temperature T_{ind} at time t with the average of the temperature instantaneous values at $t - 0.002$, $t - 0.001$, t, $t + 0.001$, and $t + 0.002$. The smoothed, instantaneous indicated temperature was then corrected for time lag and ram recovery as follows:

$$(T)_t = \left\{(T_{ind})_t + \tau\left[\frac{d(T_{ind})}{dt}\right]\right\}R$$

where

$$\tau = \frac{\tau_0[T/1000]^{-0.18}}{\sqrt{M(P_s/P_{s1})}}$$

$\tau_0 = 0.016$ and 0.021 for station 2 and the compressor interstage stations, respectively; P_s and M were obtained from the steady-state data recorded prior to each transient; X is the ram recovery factor obtained from calibration curves as a function of P_s/P; and $d(T_{ind})/dt$ is the instantaneous, indicated temperature-rise rate calculated as the slope of a least-squares straight-line curve fit of all instantaneous indicated temperatures between $t - 0.002$ and $t + 0.002$.

REFERENCES

1. Wallner, Lewis E.; Useller, James W.; and Saari, Martin J: A Study of Temperature Transients at the Inlet of a Turbojet Engine. NACA RM E 57C22, 1957.
2. Gabriel, D.S.; et al: Some Effects of Inlet Pressure and Temperature Transients on Turbojet Engines. Aeronaut. Eng. Rev., vol. 16, no. 9, Sept. 1957, pp. 54-59, 68.
3. Rudey, R.A.; and Antl, R.J.: The Effect of Inlet Temperature Distortion on the Performance of a Turbofan Engine Compressor System. NASA TM X-52788, 1970.
4. Abdelwahab, Mahmood: Effects of Temperature Transients at Fan Inlet of a Turbofan Engine. NASA TP-1031, 1977.
5. Armentrout, E.C.: Development of a High-Frequency-Response Pressure Sensing Rake for Turbofan Engine Tests. NASA TM X-1959, 1970.
6. Mazzawy, R.S.; and Banks, G.A.: Modeling and Analysis of the TF30-P-3 Compressor System with Inlet Pressure Distortion. (PWA-5302, Pratt & Whitney Aircraft; NASA Contract NAS3-18535.) NASA CR-134996, 1976.

TABLE I. - TEST CONFIGURATIONS

Experiment	Gaseous hydrogen volume, cm^3	Hydrogen-burner-heated quadrant	Hydrogen burner rotation (viewed looking upstream)	Fire valve	State of gaseous hydrogen burner prior to transient	Relative circumferential location of fan inlet (station 2, fig. 2) temperature rakes used in calculating fan inlet temperature parameters (looking upstream clockwise), deg
1	410	4	+30	A	Only pilots lit	15, 60
2	820	↓	↓	↓	↓	↓
3	1229					
4	2049					
5	2869					
6	3688					
7	4917		↓	↓		
8	2049		0	B	↓	27, 45, 63
9	2049		↓	A	Four quadrants lit plus pilots	↓
10	2049		↓	B	Four quadrants lit plus pilots	
11	3278		↓	A	Only pilots lit	
12	6146	↓	↓	↓	↓	↓
13	2868	1	+30	↓	↓	17
14	2868	2	↓			32
15	3688	2				32
16	2968	3	↓	↓	↓	32

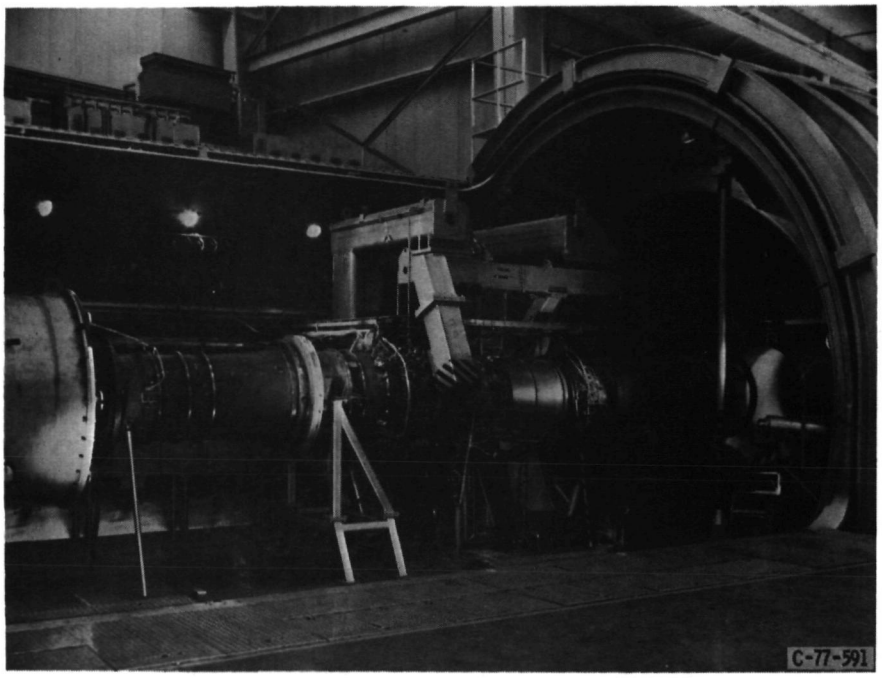

Figure 1. - TF30-P-3 engine in altitude test chamber.

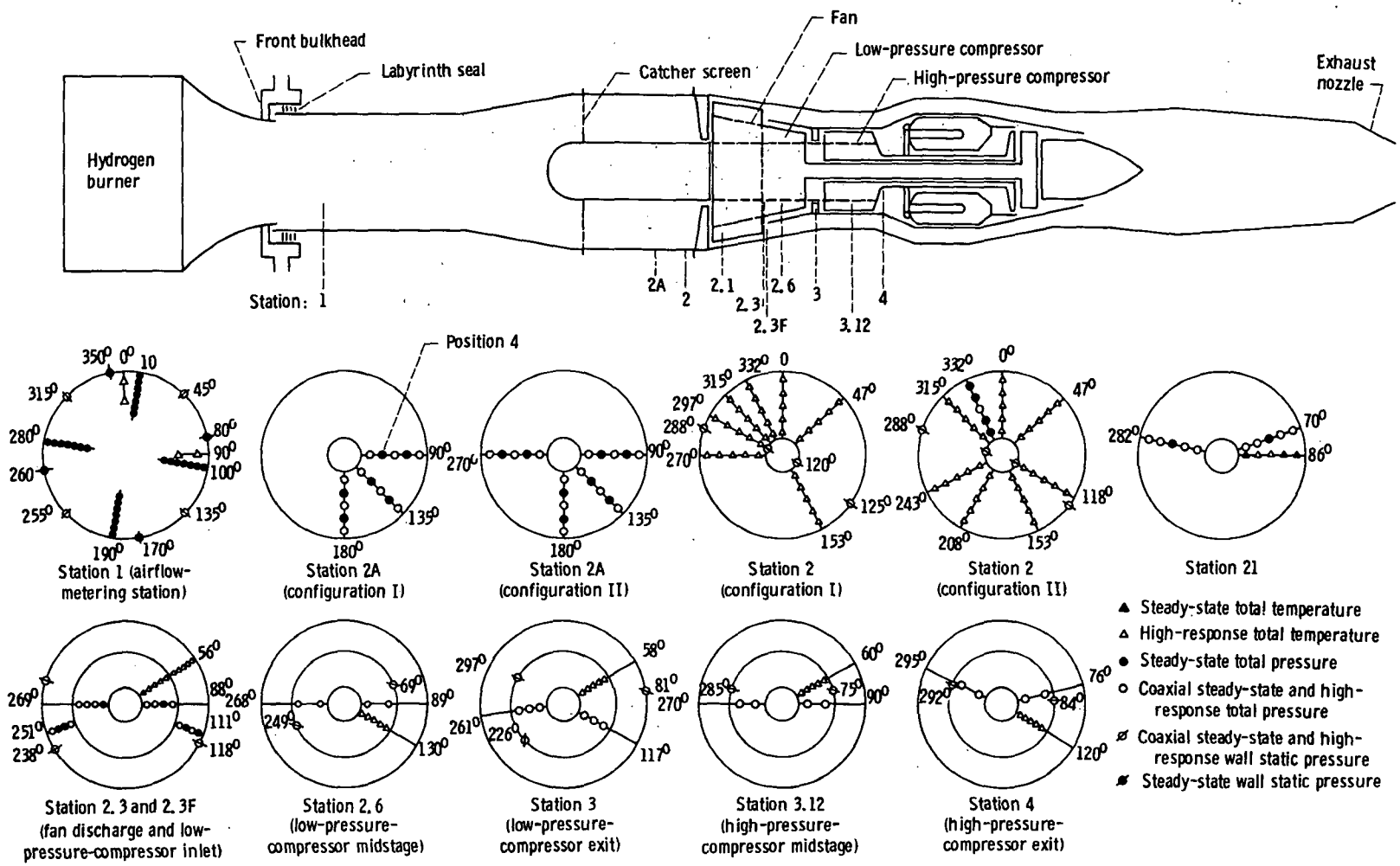

Figure 2. - Instrumentation layout for TF30-P-3 turbofan engine. (Instrumentation stations viewed looking upstream.)

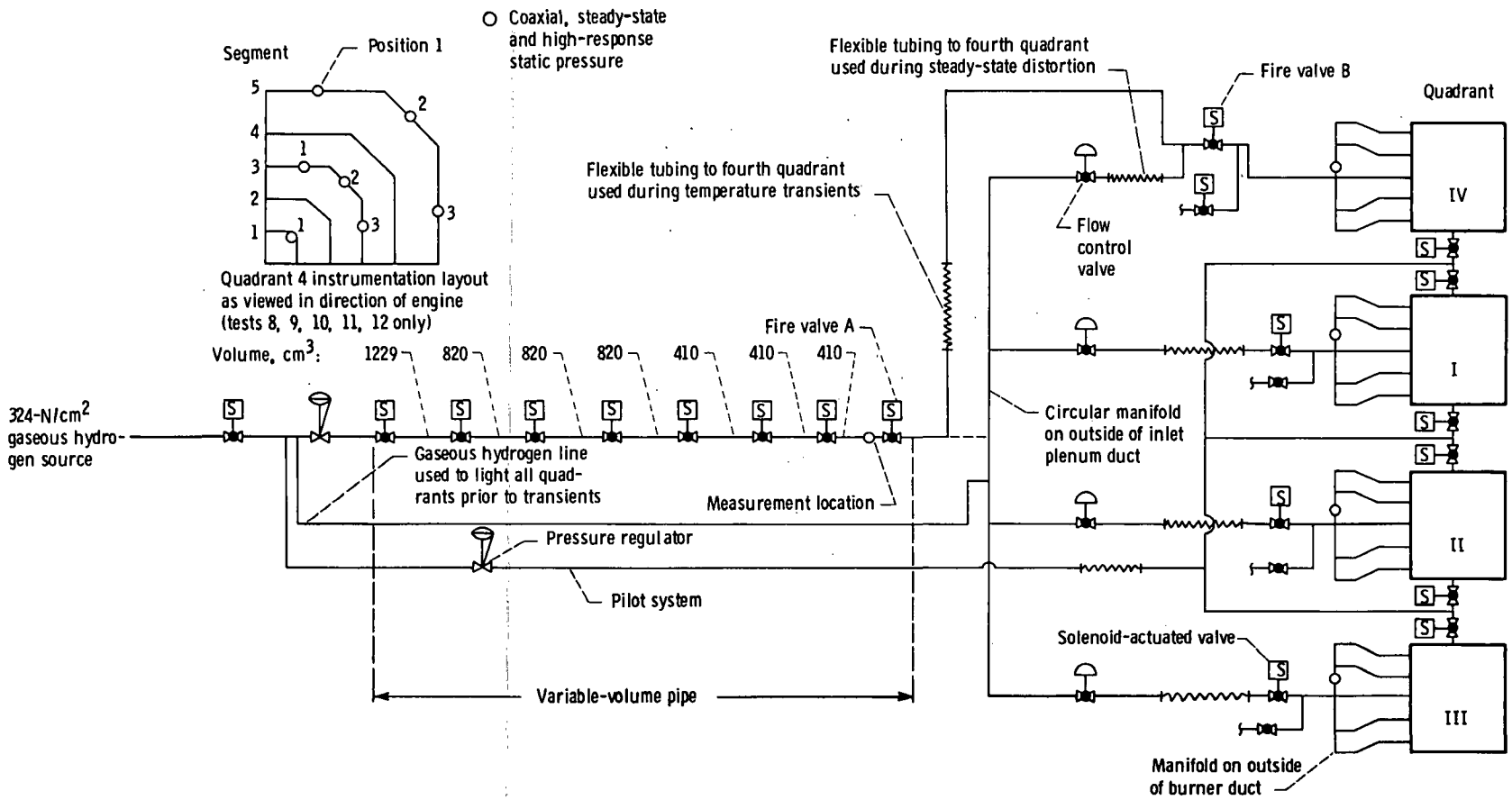

Figure 3. - Gaseous-hydrogen-fueled burner schematic and instrumentation layout.

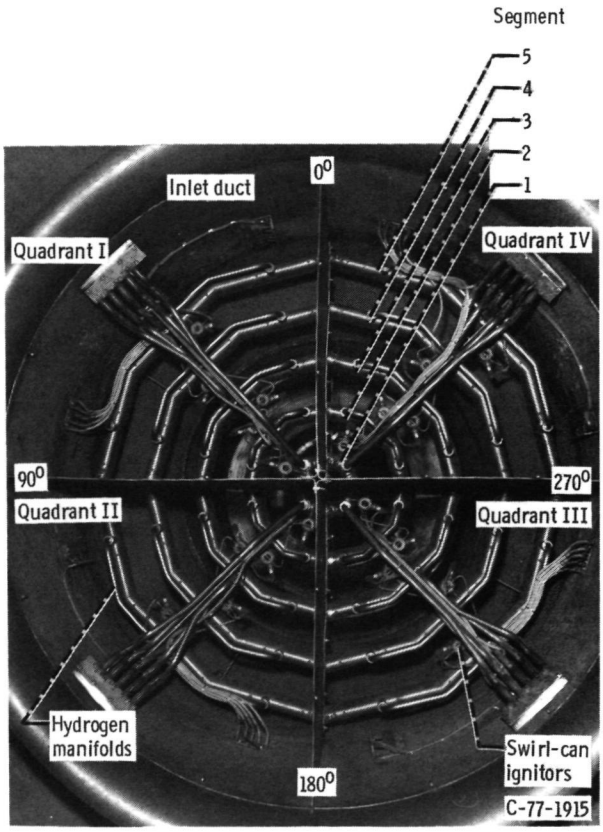

Figure 4. - Gaseous-hydrogen-fueled burner viewed in direction of engine inlet.

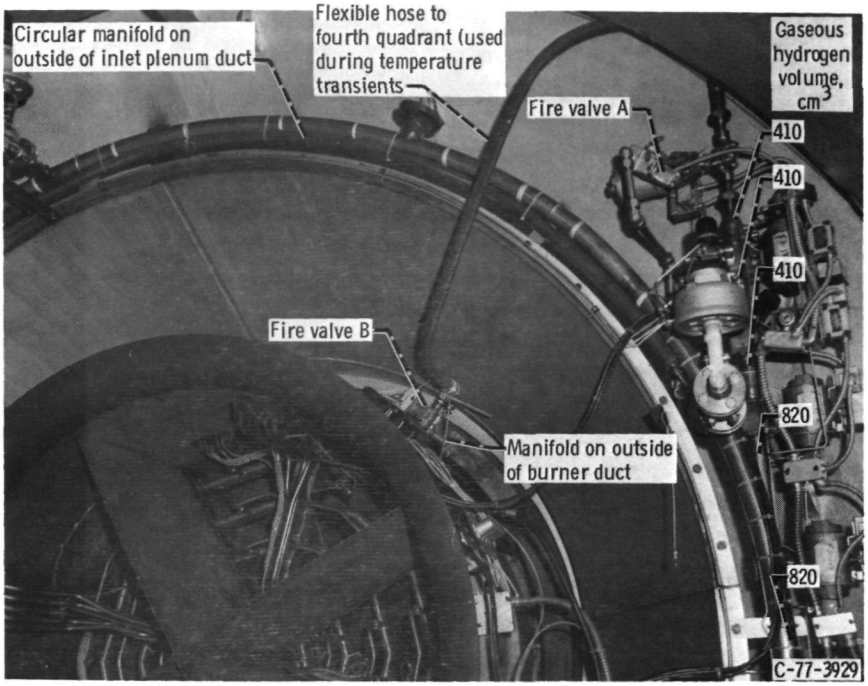

(a) For producing temperature transients.

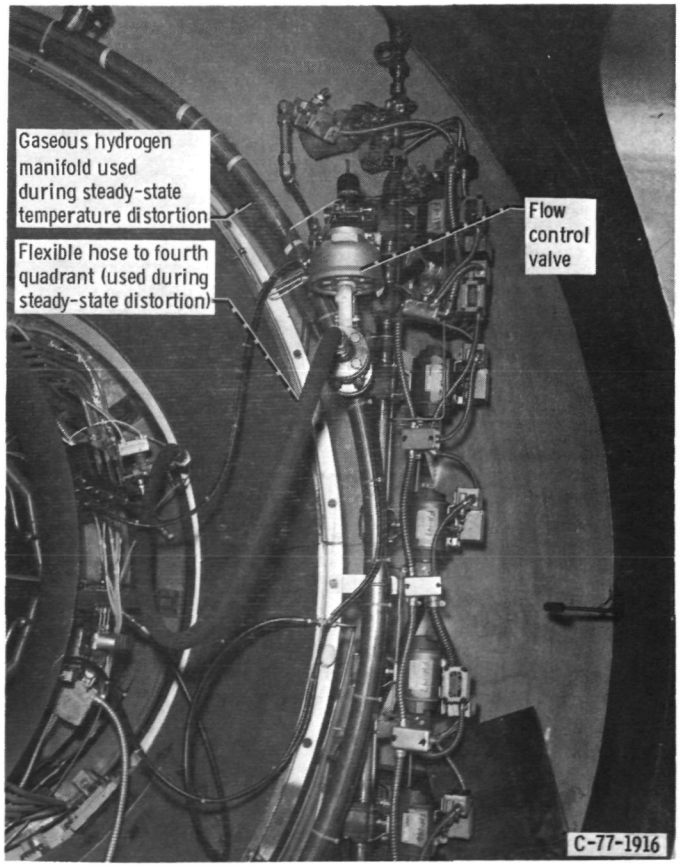

(b) For producing steady-state distortion

Figure 5. - Gaseous-hydrogen-fueled burner (quadrant IV) installation.

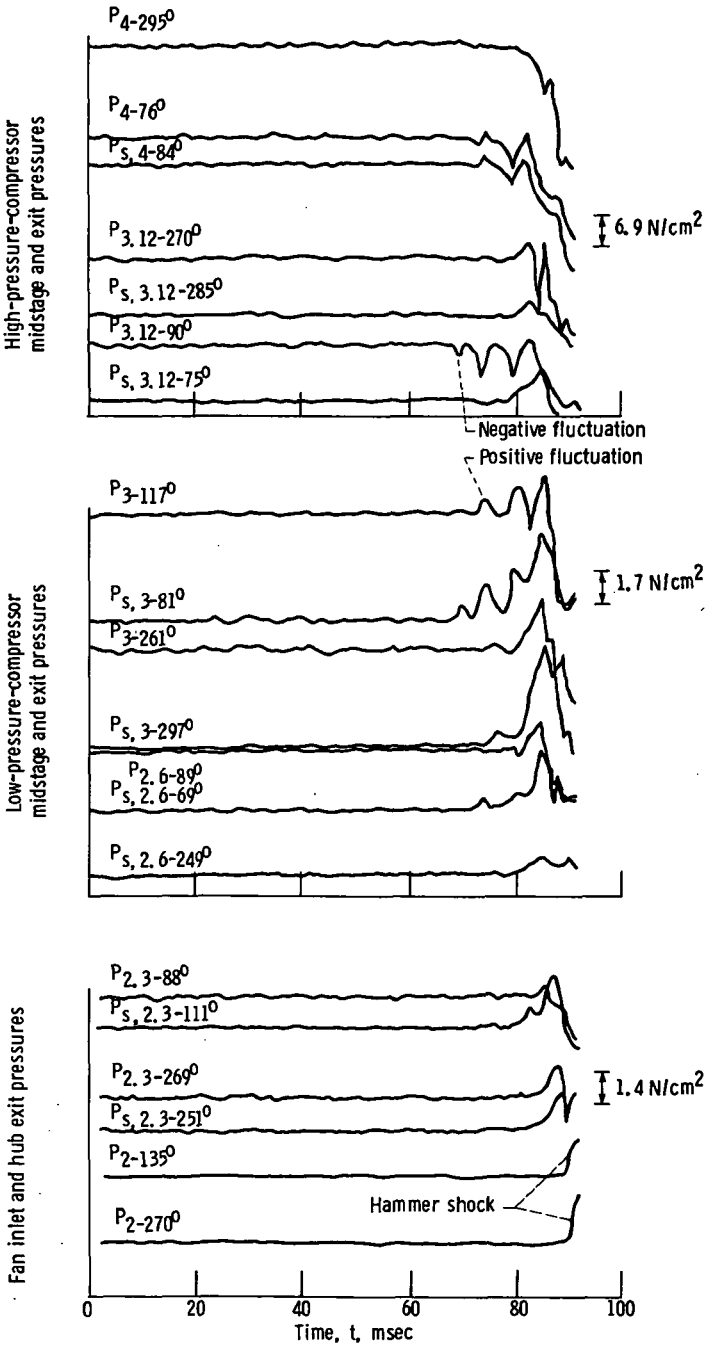

Figure 6. - Typical time history of engine pressure during steady-state temperature disturbance resulting in stall. $(\Delta T)_2$ at stall = 67 K.

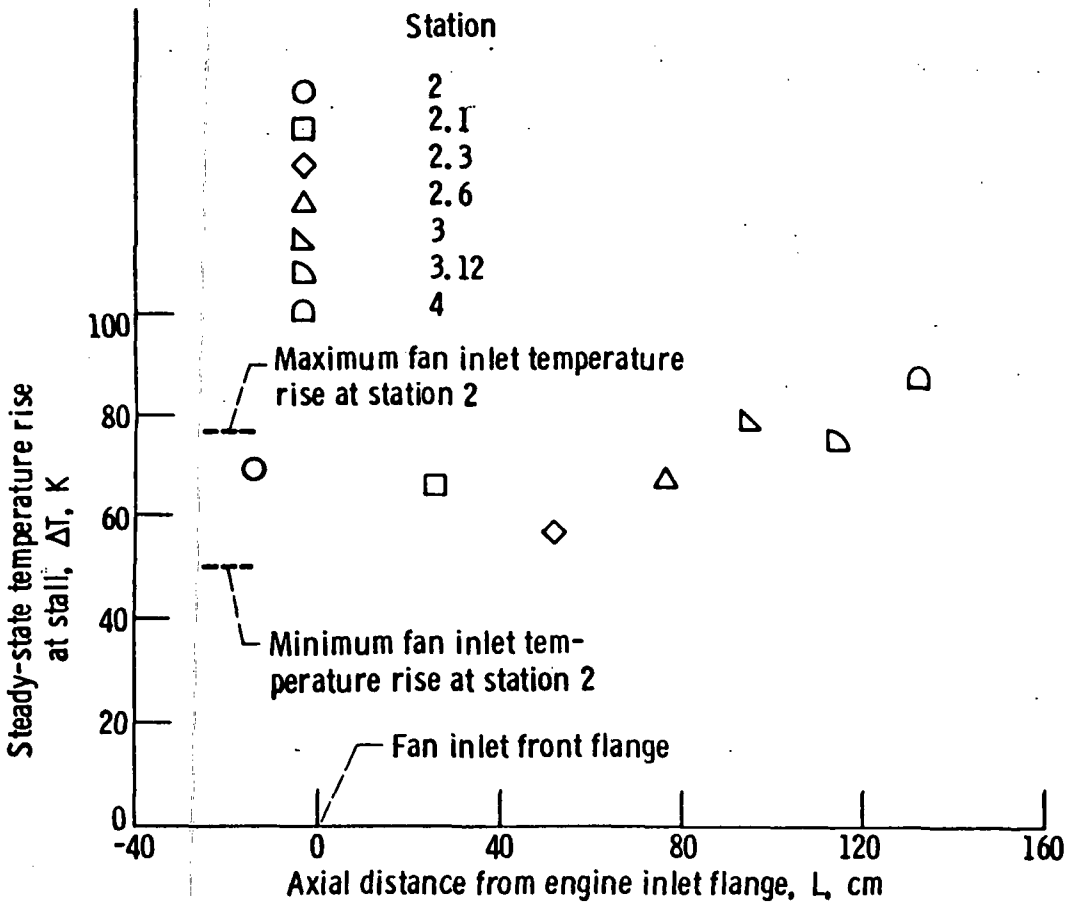

Figure 7. - Fan inlet and compression system interstage steady-state temperature rise to stall during 90°-circumferential-extent, steady-state temperature distortion.

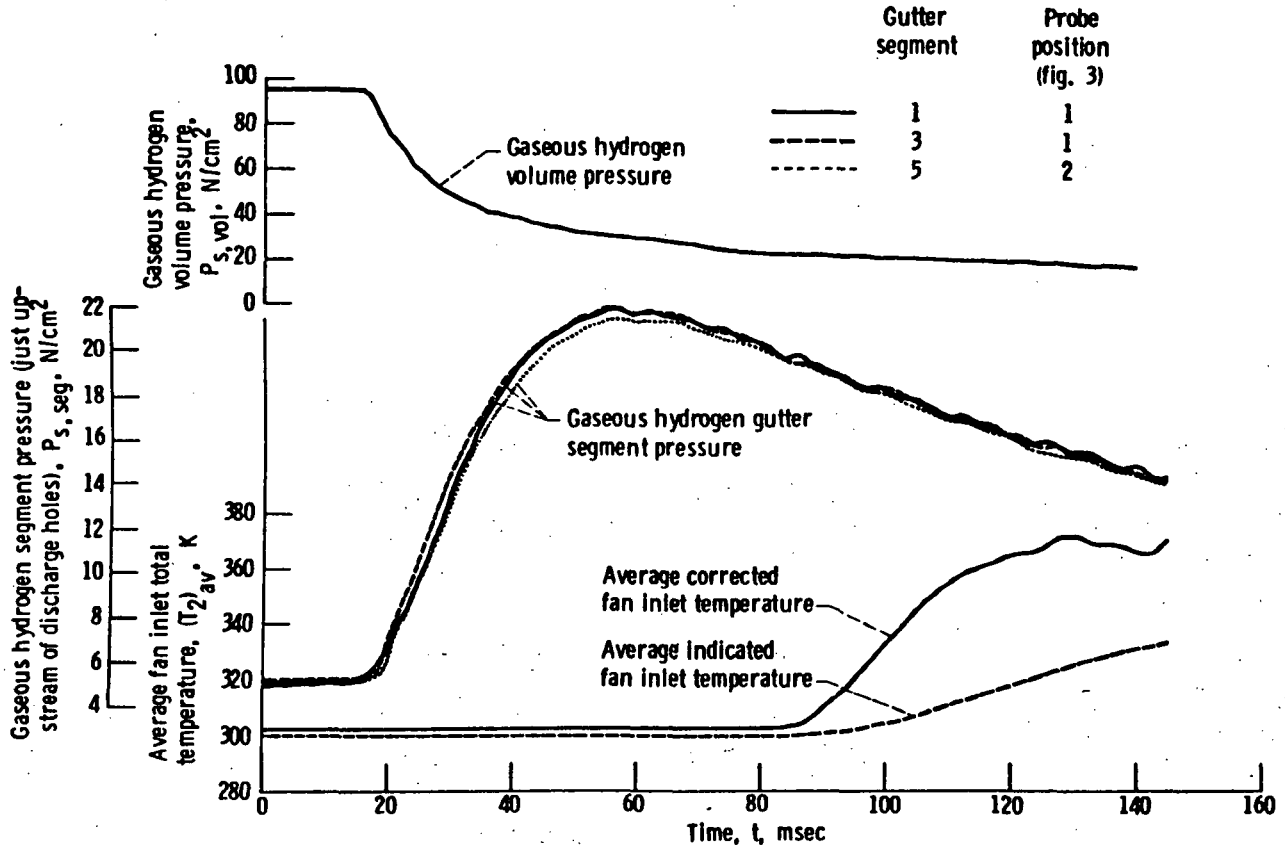

Figure 8. - Typical fan inlet temperature transient - experiment 9, quadrant IV (table I).

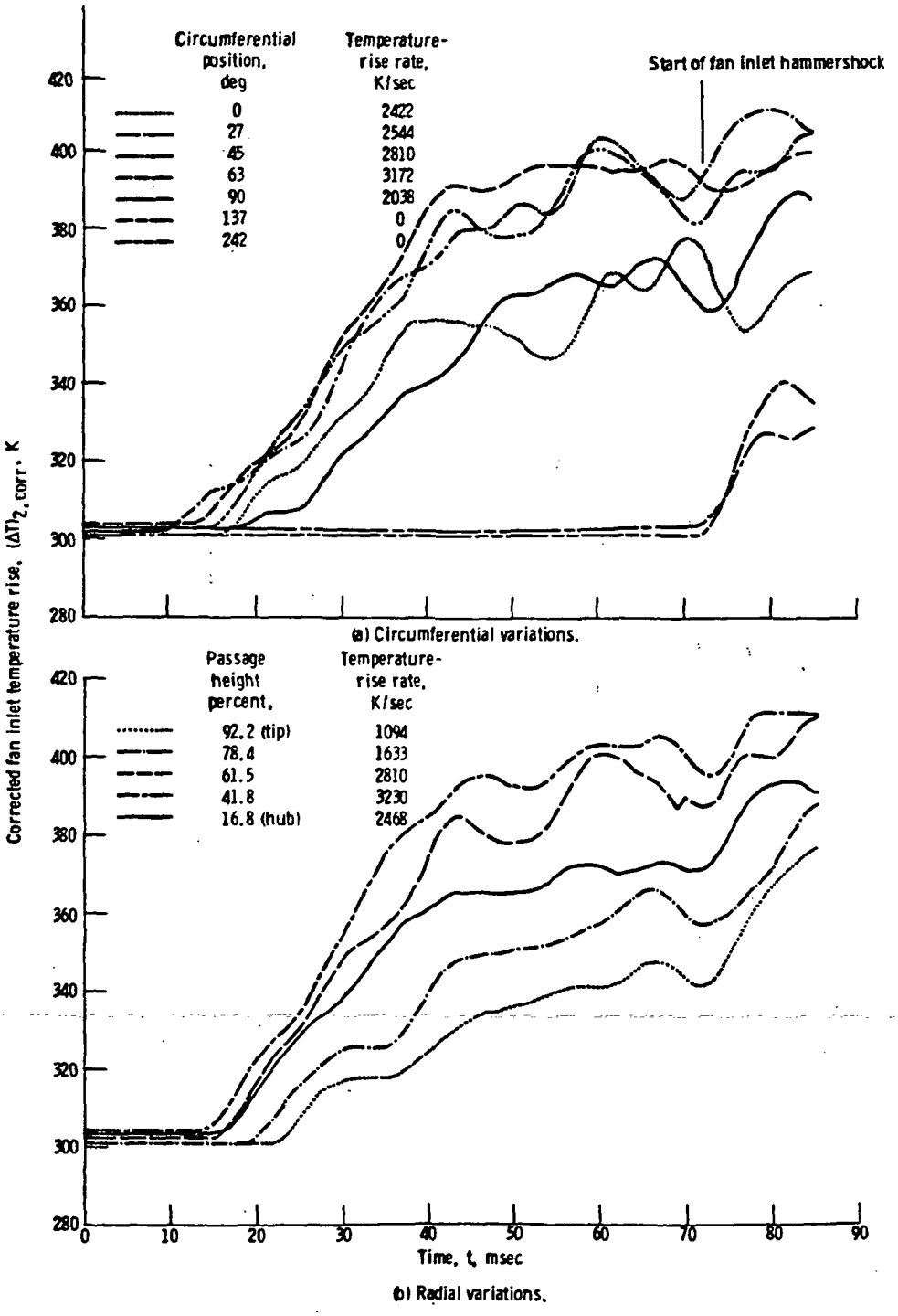

Figure 9. - Typical circumferential and radial time history of fan inlet temperature during transients. Experiment 9 (table 1.)

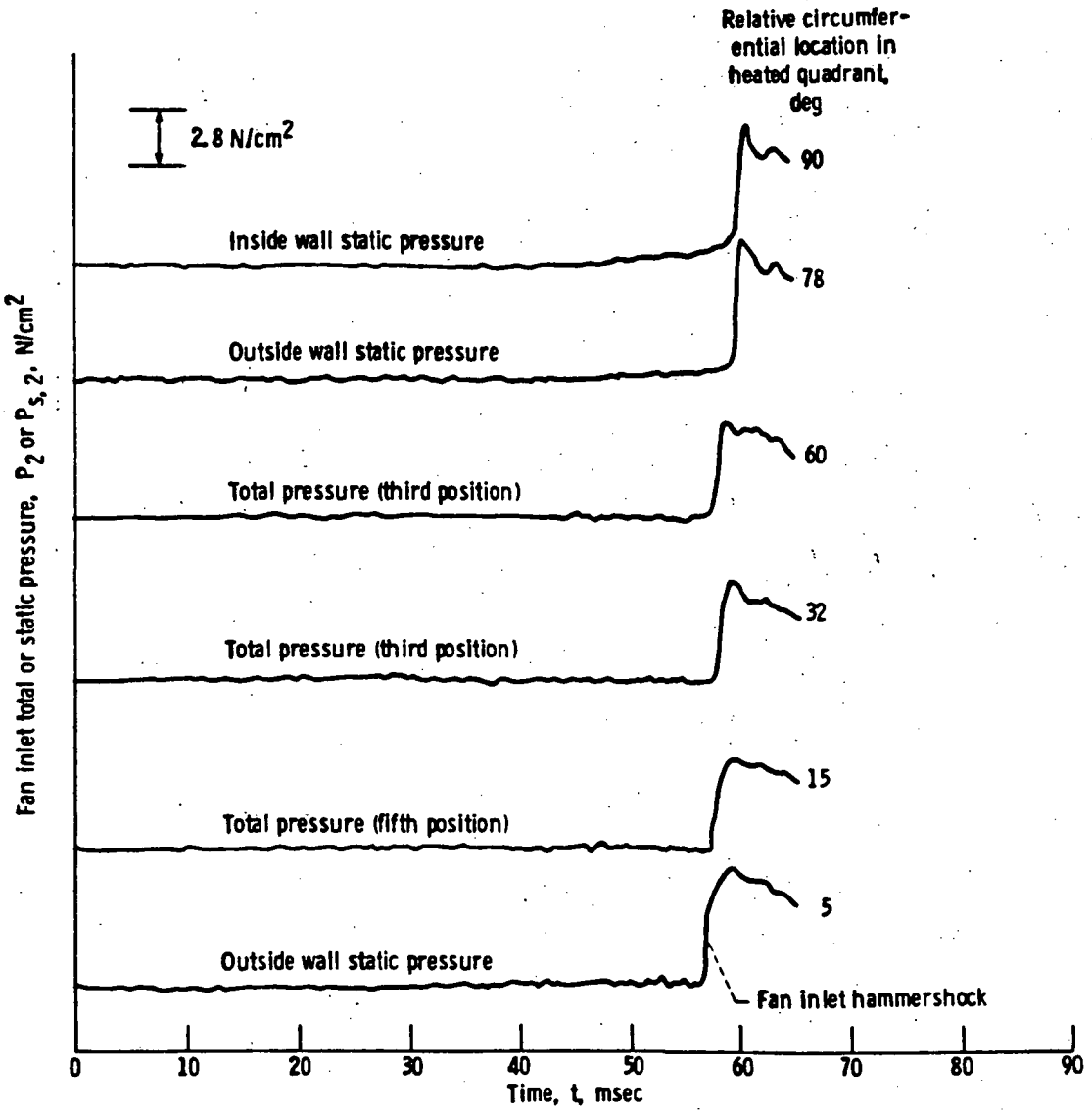

Figure 10. - Fan inlet pressure variations during temperature transients.

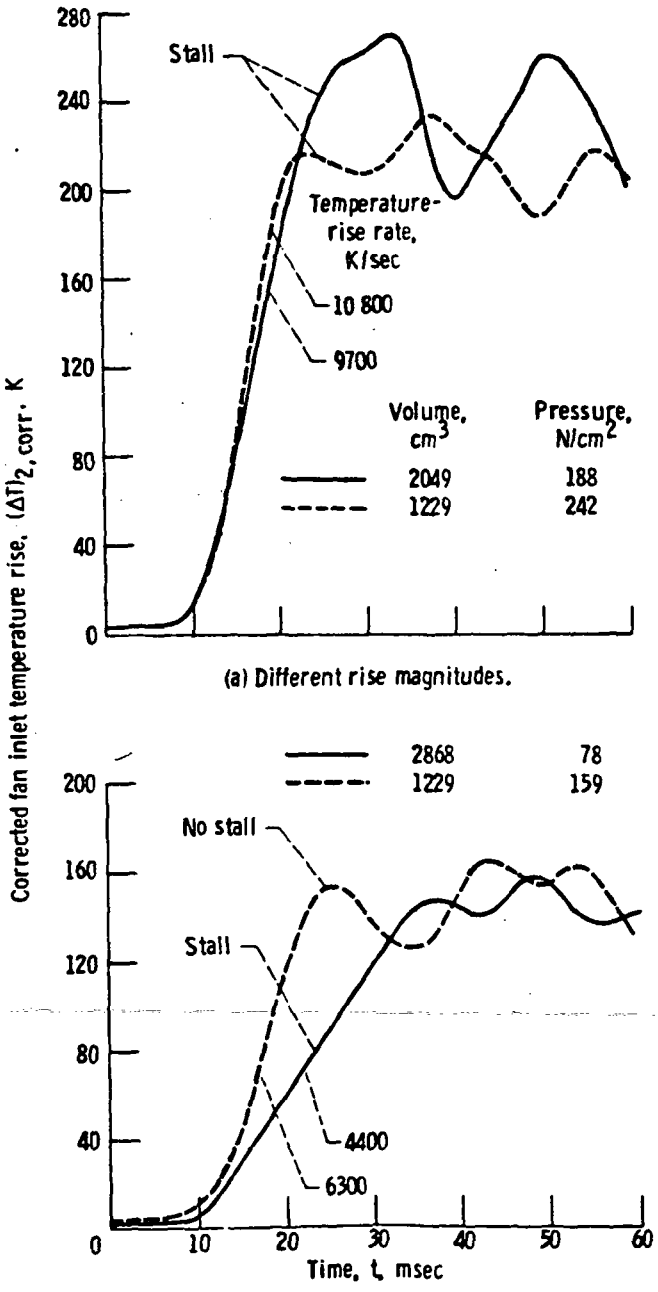

(a) Different rise magnitudes.

(b) Different rise rates.

Figure 11. - Fan inlet temperature-rise magnitude and rate as a function of gaseous hydrogen volume and pressure.

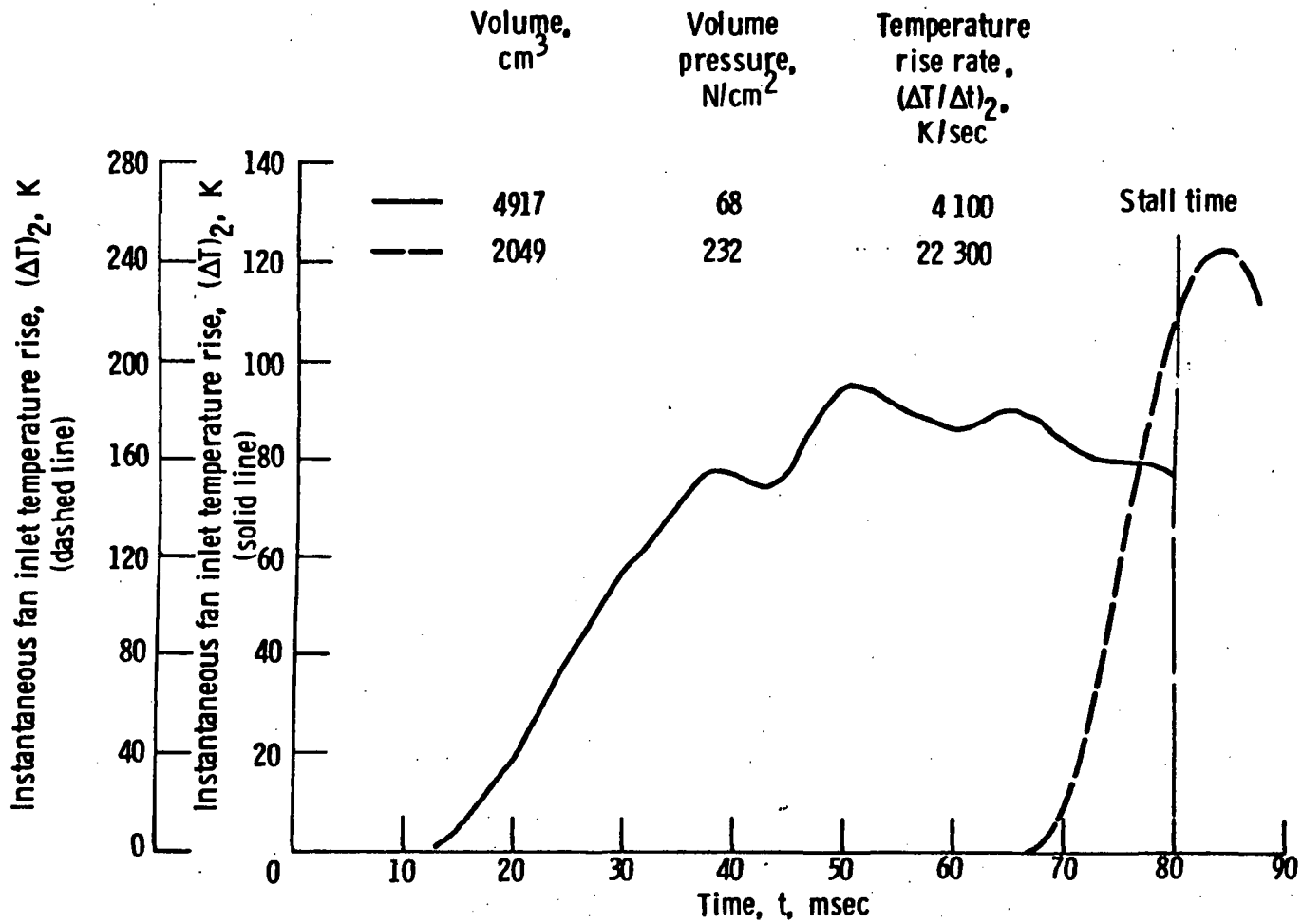

Figure 12. - Typical inlet temperature pulse types.

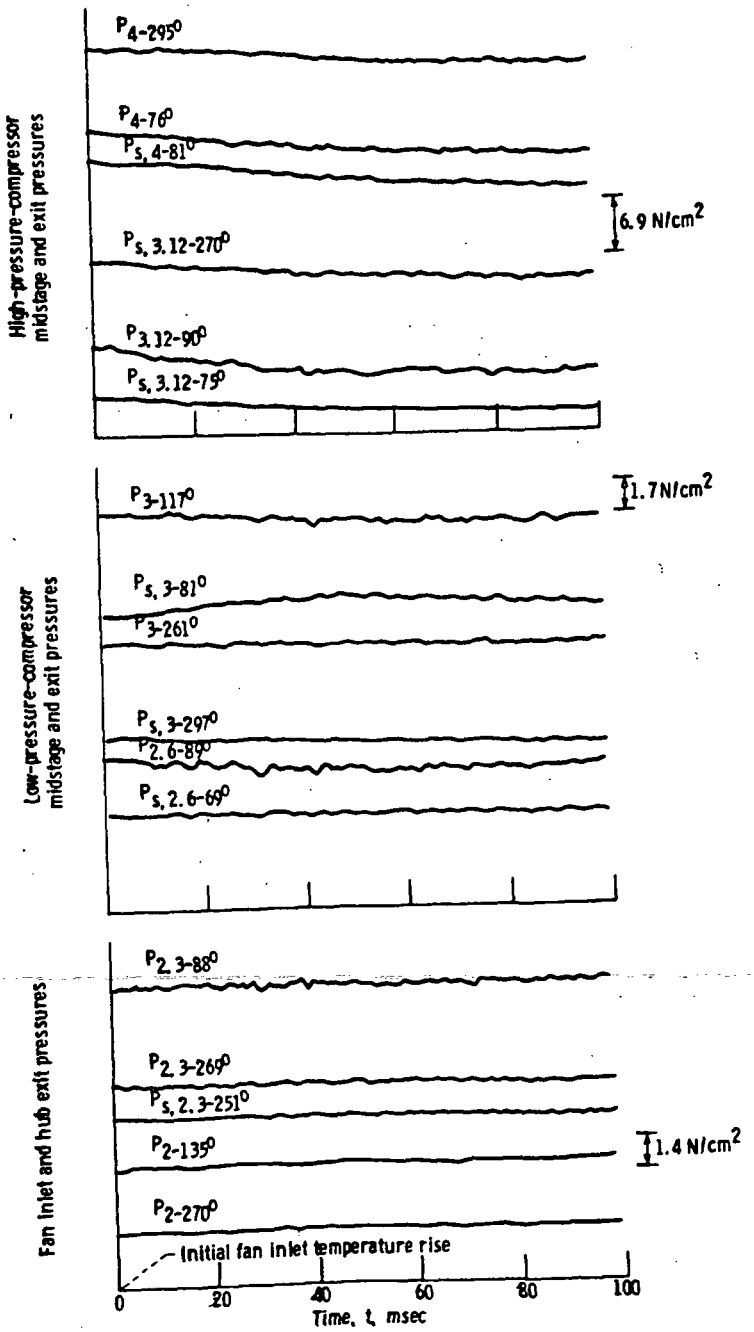

Figure 13. - Typical time history of engine pressures during time-dependent temperature distortion during which no stall occurred. Experiment 4; $(\Delta T/\Delta t)_2$ = 2900 K/sec; maximum $(\Delta T)_2$ = 65 K.

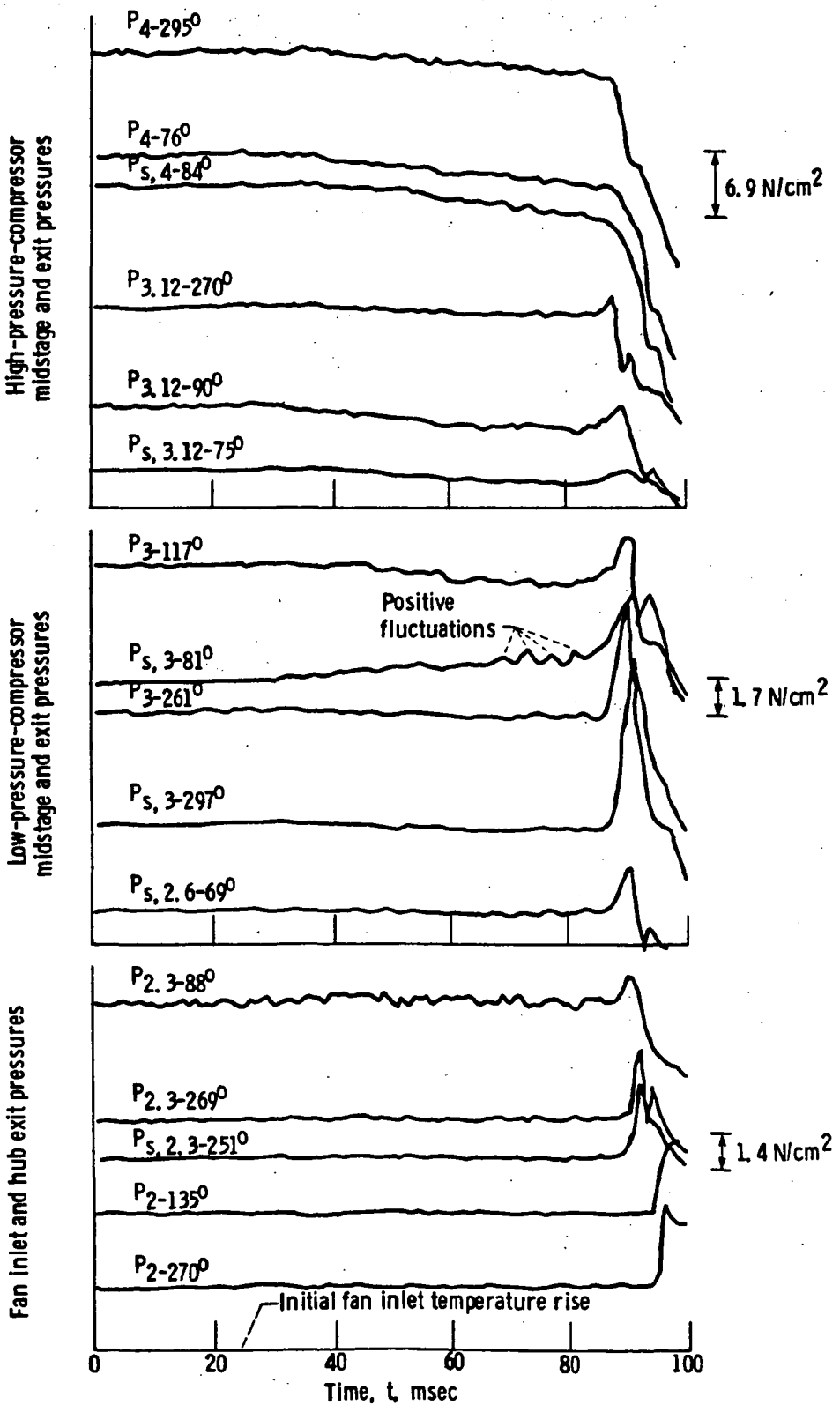

Figure 14. - Typical time history of engine pressures during time-dependent temperature distortion during which stall occurred. Experiment 7; $(\Delta T_t/\Delta t)_2$ = 4050 K/sec; $(\Delta T)_2$ at stall = 97 K.

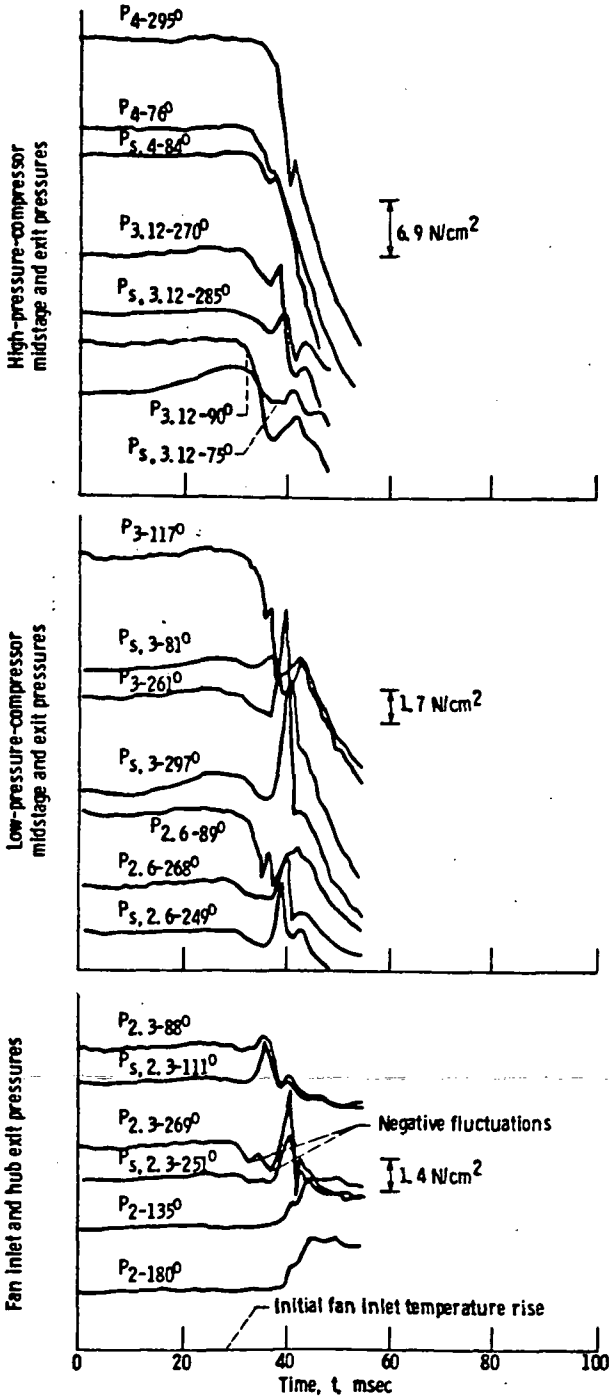

Figure 15. - Typical time history of engine pressure during time-dependent temperature distortion during which stall occurred. Experiment 8; $(\Delta T_t/\Delta t)_2$ = 22 300 K/sec; $(\Delta T)_2$ at stall = 244 K.

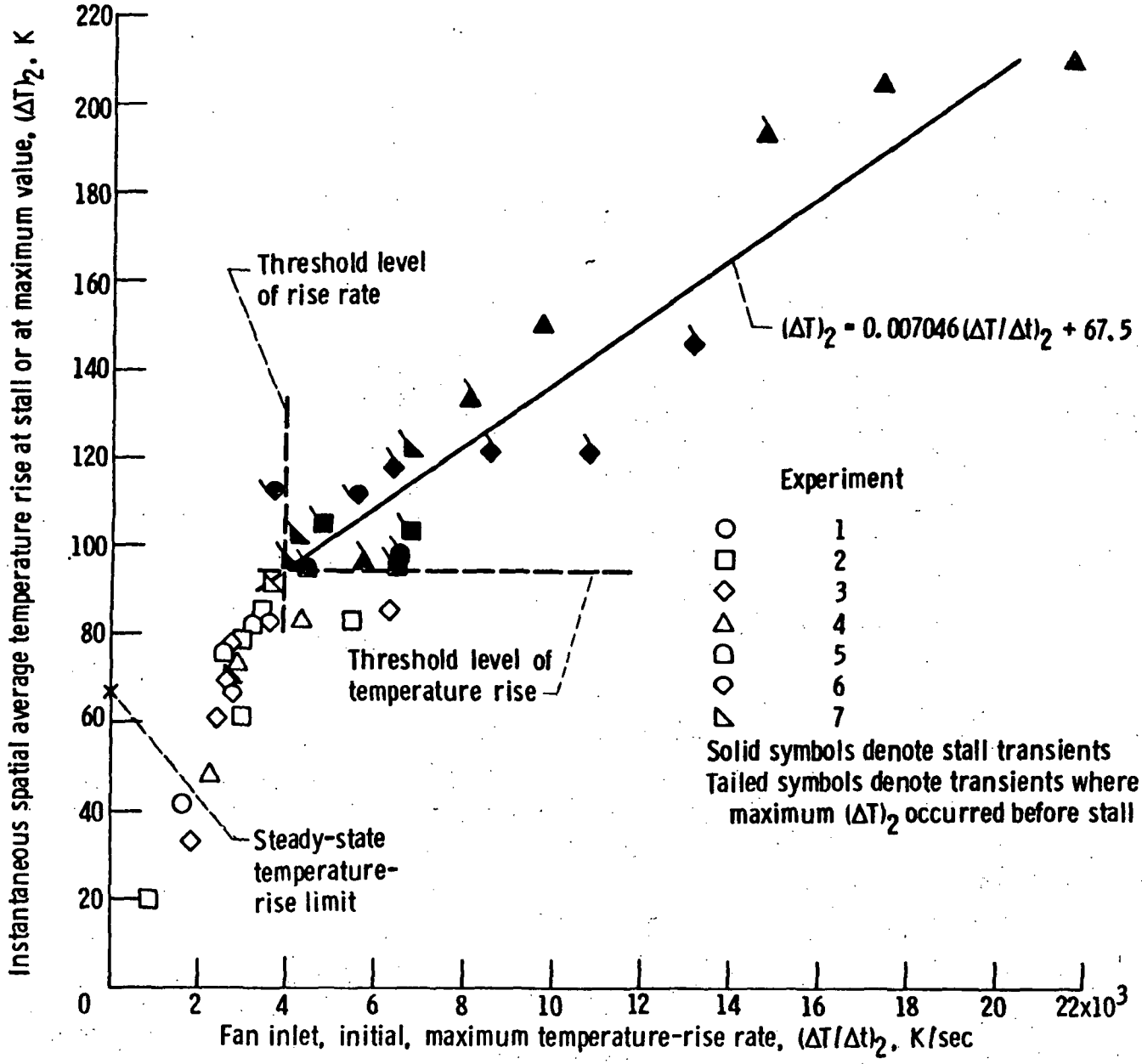

Figure 16. - Fan inlet instantaneous spatial average temperature rise as a function of initial, maximum temperature-rise rate.

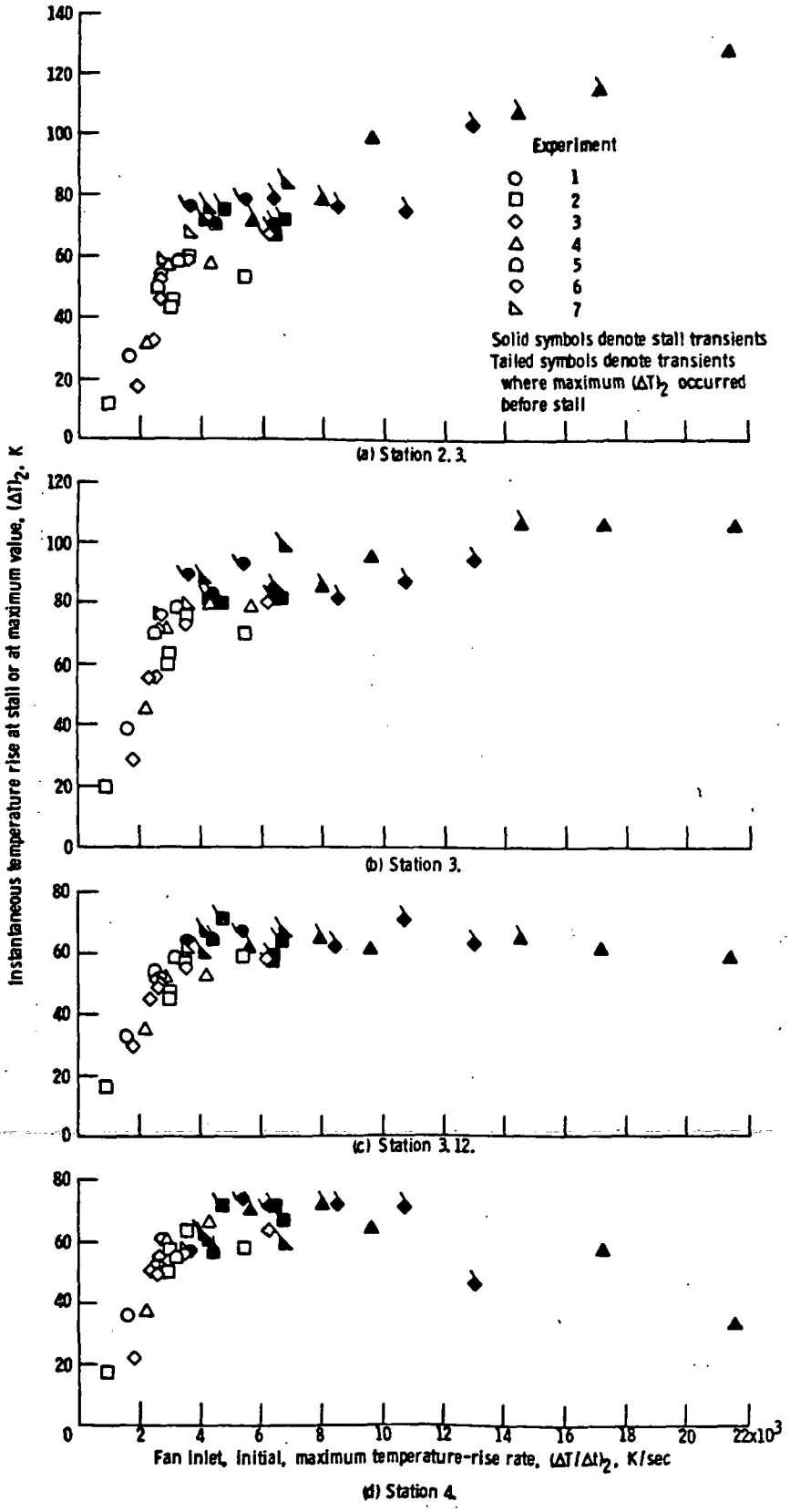

Figure 17. - Compressor interstage instantaneous temperature rise as a function of fan inlet, initial, maximum temperature-rise rate.

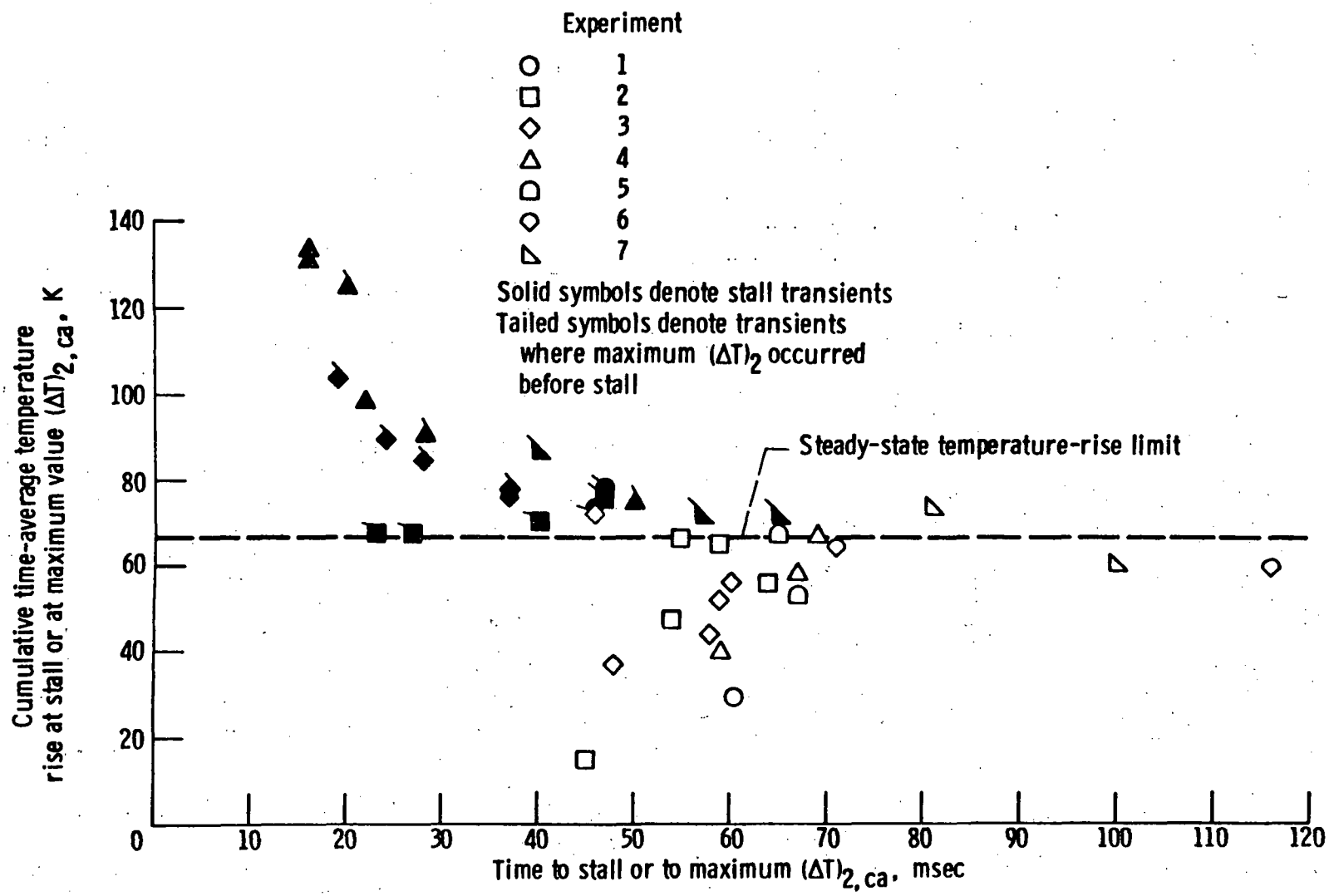

Figure 18. - Fan inlet cumulative time-average temperature rise as a function of time.

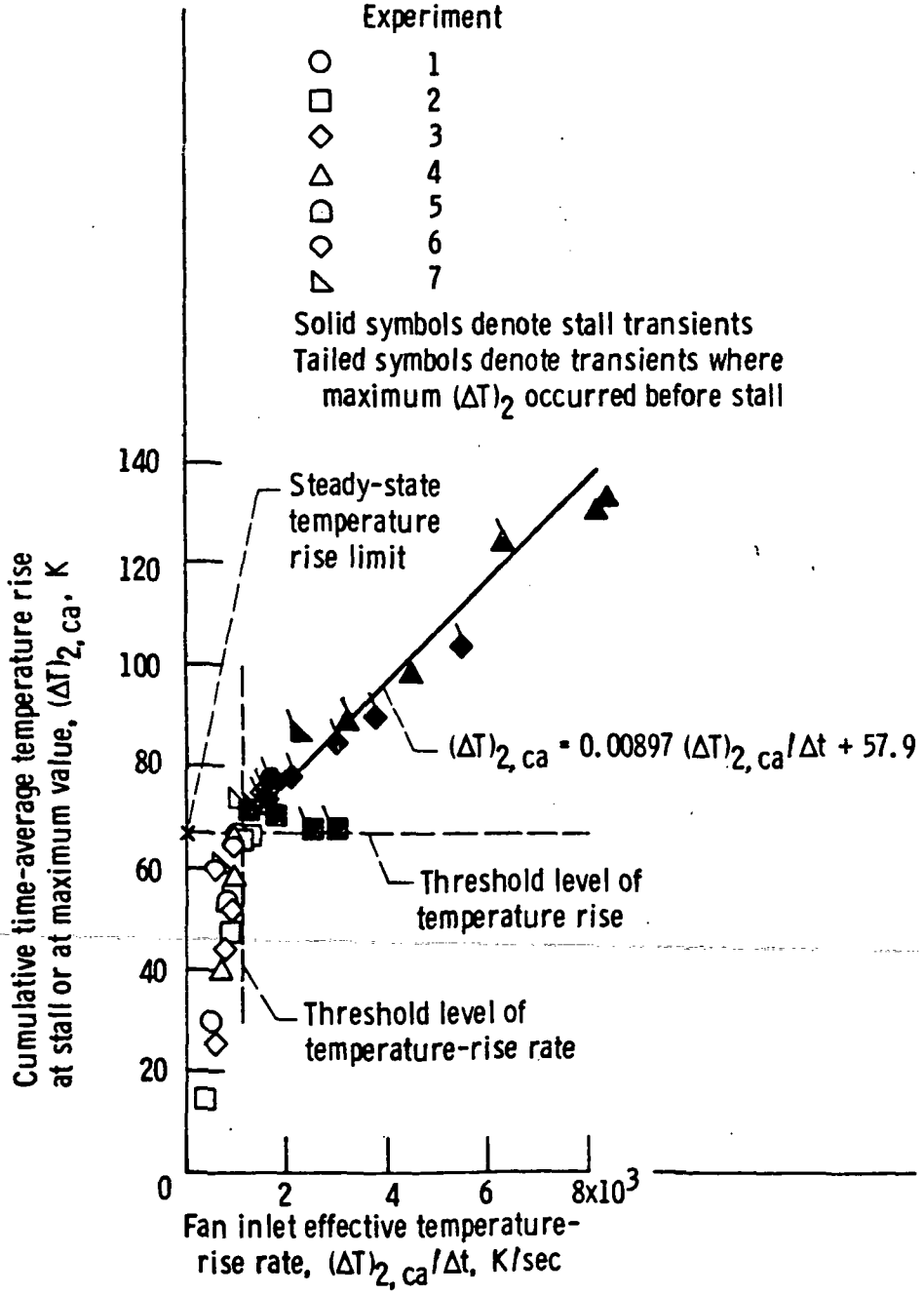

Figure 19. - Fan inlet cumulative time-average temperature rise as a function of effective temperature-rise rate.

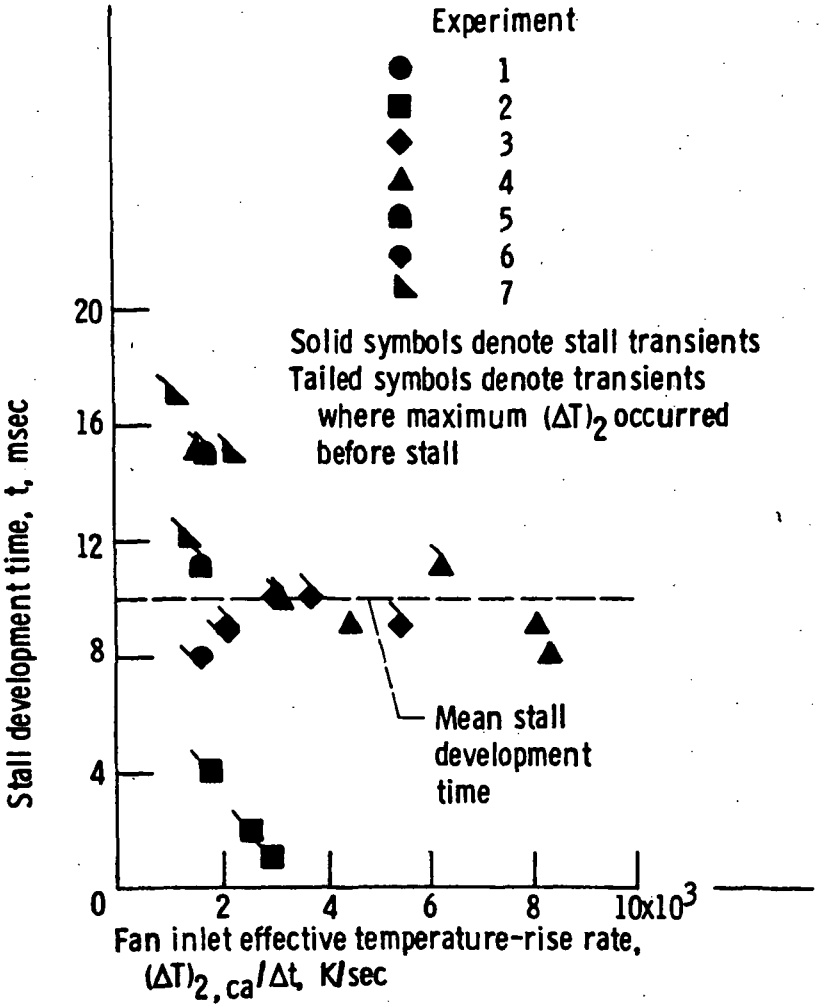

Figure 20. - Compressor stall development time as a function of effective fan inlet temperature-rise rate.

1. Report No.	2. Government Accession No.	3. Recipient's Catalog No.
NASA TM-82699		

4. Title and Subtitle	5. Report Date
EFFECTS OF FAN INLET TEMPERATURE DISTURBANCES ON THE STABILITY OF A TURBOFAN ENGINE	December 1981
	6. Performing Organization Code 505-32-6A
7. Author(s)	8. Performing Organization Report No.
Mahmood Abdelwahab	E-982
	10. Work Unit No.
9. Performing Organization Name and Address	
National Aeronautics and Space Administration Lewis Research Center Cleveland, Ohio 44135	11. Contract or Grant No.
	13. Type of Report and Period Covered
12. Sponsoring Agency Name and Address	Technical Memorandum
National Aeronautics and Space Administration Washington, D.C. 20546	14. Sponsoring Agency Code

15. Supplementary Notes

16. Abstract

An experimental investigation was conducted to determine the effects of steady-state and time-dependent fan inlet total temperature disturbances on the stability of a TF30-P-3 turbofan engine. Disturbances were induced by a gaseous-hydrogen-fueled burner system installed upstream of the fan inlet. Data were obtained at a fan inlet Reynolds number index of 0.50 and at a low-pressure-rotor corrected speed of 90 percent of military speed. All tests were conducted with a 90^{o} extent of the fan inlet circumference exposed to above-average temperatures.

17. Key Words (Suggested by Author(s))	18. Distribution Statement
Temperature disturbances; Temperature distortion; Turbofan engine: effect on stability	Unclassified - unlimited STAR Category 07

19. Security Classif. (of this report)	20. Security Classif. (of this page)	21. No. of Pages	22. Price*
Unclassified	Unclassified		

* For sale by the National Technical Information Service, Springfield, Virginia 22161

National Aeronautics and
Space Administration

Washington, D.C.
20546

Official Business
Penalty for Private Use, $300

SPECIAL FOURTH CLASS MAIL
BOOK

Postage and Fees Paid
National Aeronautics and
Space Administration
NASA-451

NASA

POSTMASTER: If Undeliverable (Section 158
Postal Manual) Do Not Return